Fortschr. Phys. **46** (1998) 6–8, 837–842

Quantum Characterization of Optical Devices

G. M. D'ARIANO and L. MACCONE

Dipartimento di Fisica 'Alessandro Volta',
via A. Bassi 6, I-27100 Pavia, Italy

Abstract

We propose an experimental procedure, based on homodyne tomography, for measuring the matrix elements of the Liouvillian of optical devices. After describing the proposed experimental setup, we give a numerical Monte-Carlo simulation of the measurement for a laser amplifier.

1. Introduction

The experiment here proposed allows the complete characterization of the quantum dynamical properties of an optical device. We show how it is possible to reconstruct the Liouvillian matrix by impinging a complete set of input states into the device and making an accurate measurement of the corresponding output states. The measurement of the output states is performed through quantum homodyne tomography [1, 2, 3]. The experimental setup is composed of a linear highly efficient photodetector, a non degenerate optical amplifier (NOPA), and a homodyne detector.

For an open quantum system the equation that evolves the density matrix ρ of radiation is given by

$$\frac{d}{dt}\,\rho(t) = \mathcal{L}[\rho(t)]\,, \qquad \mathcal{L}[\rho] \doteq -\frac{i}{\hbar}\,[H,\,\rho] + \sum_{i=0}^{N}\,\mathcal{D}[\vartheta_i]\,\rho\,, \tag{1}$$

where H is the Hermitian Hamiltonian, ϑ_i are (generally non-Hermitian) operators describing the interaction of the system with the environment, $\mathcal{L}$ is the Liouvillian superoperator, and $\mathcal{D}$ is the Lindblad superoperator

$$\mathcal{D}[\vartheta]\,\rho \doteq \vartheta\rho\vartheta^\dagger - \frac{1}{2}\,(\vartheta^\dagger\vartheta\rho + \rho\vartheta^\dagger\vartheta)\,. \tag{2}$$

In the first section of this paper we present the experimental apparatus for measuring the matrix elements of $\mathcal{L}$. In the second section we recall some notions on quantum homodyne tomography. Then, we present some Monte-Carlo simulations to test the feasibility of the experiment. Finally, in the conclusion, we give possible extensions and developments of the proposed method.

2. Experimental apparatus

The experimental apparatus depicted in Fig. 1 is capable of reconstructing the Liouvillian of devices that evolve states that are diagonal in the number representation $\rho(t) = \sum_j c_j(t)\,|j\rangle\,\langle j|$, with $|j\rangle$ eigenstate of the number operator $a^\dagger a$. Such devices are

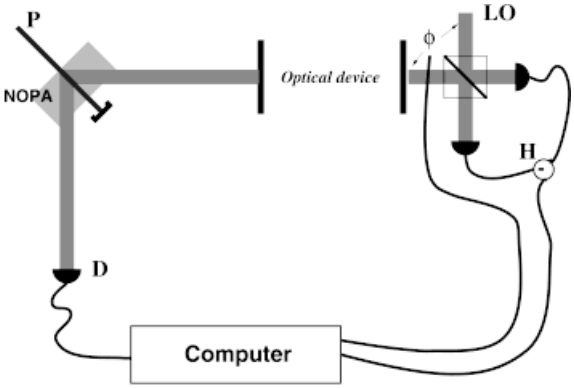

Figure 1: Sketch of the proposed experiment. The NOPA and the photodetector D are used to generate the input Fock states $\rho = |n\rangle\langle n|$. These are impinged into the device that evolves them. The Liouvillian is reconstructed through homodyne tomography of data from the homodyne detector H at the output of the device.

called "phase-insensitive", and a two-index Liouvillian matrix is needed in the number representation. The extension of the method to the measurement of generic non-diagonal four-index Liouvillian matrices for phase-sensitive devices is currently under study [4]. The non degenerate optical amplifier (NOPA) and the photodetector D, are used to create Fock states ($\rho = |n\rangle\langle n|$) to be impinged into the optical device. The NOPA with vacuum input and strong classical pump is used to create a couple of quantum correlated twin-beams. The state of the radiation at the output of the NOPA is [5]

$$|\psi\rangle = \sqrt{1 - |\kappa|^2} \sum_{n=0}^{\infty} \kappa^n |n\rangle\,|n\rangle\,, \tag{3}$$

where κ is the pump–parameter. At detector D the number of photons in one of the two beams is measured, and, because of the quantum correlations between the beams, for unit quantum efficiency $\eta_D = 1$ at D the other beam is projected onto the eigenstate $|n\rangle$ of the number of photons, n being the value detected at D. In the more realistic case of non-unit quantum efficiency $\eta_D < 1$ the detector D is equivalent to a perfect detector preceded by a beam splitter of transmissivity η_D. In this case the state reduction yields the mixture

$$\rho_n = \sum_{k=n}^{\infty} D_{nk}\,|k\rangle\langle k|, \qquad D_{nk} \doteq \frac{[|\kappa|^2(1-\eta_D)]^{k-n}\,k!}{\mathcal{N}(k-n)!}\,, \tag{4}$$

where n is the result of the measurement at the detector D, and $\mathcal{N}$ is a normalization factor. The evolution of the state through the optical device is governed by the master equation (1) which is solved by the Green superoperator $\mathcal{G}^{(t)} \doteq \exp(t\mathcal{L})$, where t is the evolution time. The matrix elements of the Green superoperator are reconstructed by determining the state ρ_{out} at the output of the device through a homodyne tomography performed at detector H. For phase-insensitive devices the two-index matrix of the Green superoperator $\mathcal{G}^{(t)}$ is given by

$$G^{(t)}_{mn} \doteq \langle m|\,\mathcal{G}^{(t)}[|n\rangle\langle n|]\,|m\rangle\,. \tag{5}$$

The photon number probability distribution at the output of the optical device is the n-th row of the Green matrix $G^{(t)}_{mn}$, where n is the number of photons detected at detector D. In fact, the output state is

$$\rho_{out} = \mathcal{G}^{(t)}[|n\rangle\langle n|] = \sum_{m=0}^{\infty} p_n(m)\,|m\rangle\langle m|\,, \tag{6}$$

so that, for the matrix elements $G^{(t)}_{mn}$, one has the identity

$$G^{(t)}_{mn} = p_n(m)\,. \tag{7}$$

The Liouvillian can now be obtained by taking the natural logarithm [6] of the matrix $G^{(t)}_{mn}$, namely $L_{mn} = \frac{1}{t}[\log\,(G^{(t)})]_{mn}$. In the case of non-unit quantum efficiency $\eta_D < 1$ at detector D, if the photon number n is detected, the k-th row is chosen at random according to the probability distribution D_{nk} in Eq. (4).

3. Quantum homodyne tomography

In this section we recall some details of the theory of quantum homodyne tomography. For strong classical local oscillator (LO) the balanced homodyne detector H in Fig. 2 measures the quadrature $a_\phi = \frac{1}{2}(a^\dagger e^{i\phi} + a e^{-i\phi})$ of the field, where ϕ is the phase of the input mode a relative to the LO. For non-unit quantum efficiency η at photodetectors P_1 and P_2, one has an added Gaussian noise with variance $\Delta^2_\eta = \frac{1-\eta}{4\eta}$.

Homodyne tomography is an experimental technique that allows the measurement of the density matrix of the radiation state from homodyne measurements. For quantum efficiency η one can recover the density matrix of the state as [2]

$$\rho = \int_0^\pi \frac{d\phi}{\pi} \int_{-\infty}^{+\infty} dx\; p_\eta(x,\,\phi)\, K_\eta(x - a_\phi)\,, \tag{8}$$

where $p_\eta(x,\,\phi)$ is the probability distribution of homodyne data and the kernel $K_\eta(x)$ is given by

$$K_\eta(x) = \frac{1}{2}\,\mathrm{Re} \int_0^{+\infty} dk\; k e^{\frac{1-\eta}{8\eta}k^2 + ikx}\,, \tag{9}$$

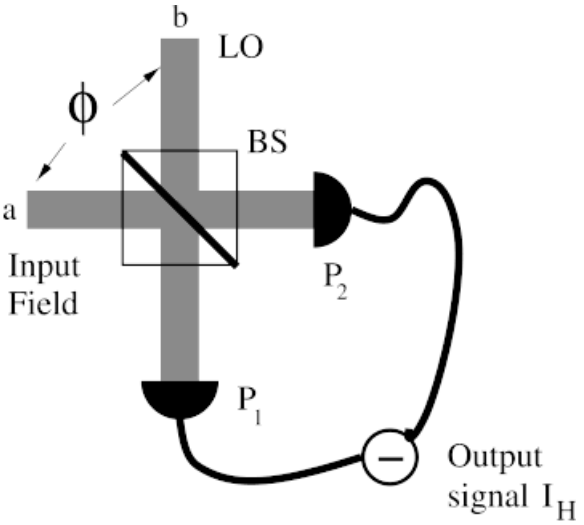

Figure 2: Sketch of the homodyne detector. The input radiation a to be measured impinges into a 50% beam splitter BS, where it is combined with the local oscillator mode b, at phase ϕ relative to the input field. The measurement result is the difference between the photocurrents measured at the two photodectors P_1 and P_2 rescaled by the amplitude of the field of the LO. In this way the homodyne detector measures the quadrature $a_\phi \doteq 1/2(ae^{-1\phi} + a^{i\phi})$ of the input field mode.

and for $\eta = 1$ (ideal photodetection) becomes

$$K(x) = -\frac{1}{2}\,\mathcal{P}\,\frac{1}{x^2}\,, \tag{10}$$

with $\mathcal{P}$ denoting the Cauchy principal value. For any two vectors $|\xi\rangle$ and $|\zeta\rangle$ in the Hilbert space such that $\langle\xi|\,K_\eta(x-a_\phi)\,|\zeta\rangle$ is bounded for all x and ϕ, one can statistically sample the matrix element $\langle\xi|\,\rho\,|\zeta\rangle$, through Eq. (8). In fact, for bounded $\langle\xi|\,K_\eta(x-a_\phi)\,|\zeta\rangle$, the central limit theorem guarantees that

$$\int_0^\pi \frac{d\phi}{\pi} \int_{-\infty}^{+\infty} dx\; p_\eta(x,\,\phi)\,\langle\xi|\,K_\eta(x-a_\phi)\,|\zeta\rangle = \lim_{N\to\infty}\frac{1}{N}\sum_{n=0}^{N}\langle\xi|\,K_\eta(x_n-a_{\phi_n}))\,|\zeta\rangle\,, \tag{11}$$

where $\{(x_n,\,\phi_n)\}$ are the homodyne outcomes at random values ϕ_n of the phase ϕ relative to the LO. For finite N the estimate (12) of the integral is Gaussian distributed around the true value, with error decreasing as $N^{-1/2}$. In the present paper we will consider only the number-state representation, and in this case $\langle n|\,K_\eta(x-a_\phi)\,|m\rangle$ is bounded for $\eta > \frac{1}{2}$ [2].

4. Numerical simulation

In this section we present a numerical Monte-Carlo simulation of the measurement of the Liouvillian of a one-atom laser amplifier, which is a relevant case of a phase-insensitive device. The laser's master equation is [7]

$$\frac{d}{dt}\,R = \left\{\frac{\gamma_\parallel}{2}\,(1+\sigma_0)\,\mathcal{D}[\sigma_+] + \frac{\gamma_\parallel}{2}\,(1-\sigma_0)\,\mathcal{D}[\sigma_-]\right.$$
$$\left. + \frac{1}{2}\left(\gamma_\perp - \frac{\gamma_\parallel}{2}\right)\mathcal{D}[\sigma_z] + \gamma\mathcal{D}[a]\right\} R + g[\sigma_+ a - \sigma_- a^\dagger,\, R] \tag{12}$$

where g is the electrical-dipole coupling, $\gamma_\parallel$ and $\gamma_\perp$ are the decay rates of population inversion and atomic polarization respectively, γ is the cavity decay rate, σ_0 is the unsaturated

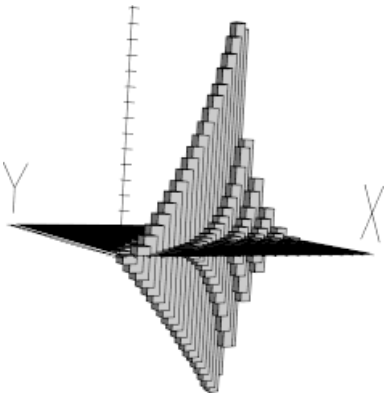

Figure 3: Theoretical Liouvillian for an one-atom laser, obtained by solving the master equation (14) by the quantum-jump method. The parameters for this laser are $C \doteq \frac{g^2}{\gamma\gamma_\perp} = 20$; $n_s \doteq \frac{\gamma_\parallel\gamma_\perp}{4g^2} = 0.5$; $\sigma_0 = 1$; $f = \frac{\gamma_\parallel}{2\gamma_\perp} = 1$; $\gamma = 1$.

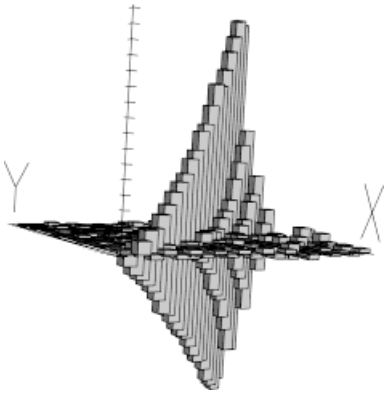

Figure 4: Monte-Carlo simulated experiment for the reconstruction of the laser theoretical Liouvillian in Fig. 3. Five statistical blocks of 4000 homodyne data for each output state have been used.

inversion ($-1 \leq \sigma_0 \leq 1$), $\sigma_{\pm,z}$ are the Pauli matrices (with 0, ± 1 entries) and R denotes the joint atom-radiation density matrix. The result of the tomographic measurement is the effective Liouvillian that evolves only the reduced radiation density matrix ρ, with the atomic degrees of freedom traced out after a "flying" time t_*.

The theoretical Liouvillian for the sole radiation cannot be obtained analitically from Eq. (14), and here for a precise evaluation we use a quantum-jump simulation [8] based on a large set of quantum histories. The result is shown in Fig. 3.

Once the theoretical Green matrix G_{nm} is evaluated, we simulate the experiment as follows. For any Fock state $\rho_{in} = |j\rangle\langle j|$ impinging into the laser we have the output state $\rho_{out} = \sum_m G^{(t)}_{mn}|m\rangle\langle m|$ as in Eq. (7), and then we simulate the output photocurrent at the homodyne detector H. In this way we have the simulated experimental data for the tomographic reconstruction based on Eq. (12), from which we measure the Green matrix $G^{(t)}_{mn}$ and the Liouvillian L_{mn}. The procedure is repeated on many statistical samples in order to evaluate the statistical errors of the matrix elements L_{mn}.

In Fig. 4 the reconstruction of the laser Liouvillian, is given as it would appear from the proposed experiment for unit quantum efficiencies $\eta_D = \eta_H = 1$. This should be compared to Fig. 3, where the theoretical Liouvillian is represented. Notice how the details of the Liouvillian are recovered for just 4×10^5 data. In Fig. 5 the statistical errors are reported for some non-zero diagonals of the Liouvillian matrix.

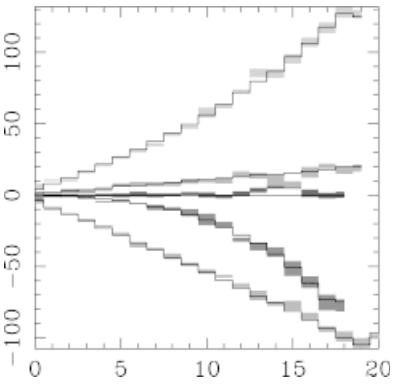

Figure 5: Some of the non-zero diagonals of the laser Liouvillian are plotted with the error bars. The full line is the theoretical Liouvillian coming from the quantum jump numerical solution as given in Fig. 3.

5. Conclusion

In this paper we proposed an experimental method for reconstructing the Liouvillian superoperator of phase insensitive devices, a large class of devices including laser amplifiers. A numerical Monte-Carlo simulation for a one-atom laser has been presented. The practical realization of the proposed experiment is connected with the availability of a linear and efficient photodetector to be used at D in the setup in Fig. 1. With the current technology [9] it seems that such a detector should be available in the next few years. We are currently working on the extension of the method for measuring phase-sensitive Liouvillian matrices on one hand, and for reducing errors from the non-unit quantum efficiency on the other hand. Notice that the effect of non-unit quantum efficiency at detector H is already taken into account in Eq. (12).

The possibility of achieving the measurement experimentally is of practical interest for the forthcoming technology of quantum gates and for novel full-optical devices that will perform digital signal processing directly on radiation at the quantum level.

References

[1] G. M. D'ARIANO, C. MACCHIAVELLO, and M. G. A. PARIS, Phys. Rev. A **50**, 4298 (1994).
[2] G. M. D'ARIANO, U. LEONHARDT, and M. PAUL, Phys. Rev. A **52** R1881 (1995).
[3] U. LEONHARDT, M. MUNROE, T. KISS, TH. RICHTER, and M. G. RAYMER, Opt. Comm. **127**, 144 (1996); S. SCHILLER, G. BREITENBACH, S. F. PEREIRA, T. MÜLLER, and S. MLYNEK, Phys. Rev. Lett. **77**, 2933 (1996).
[4] G. M. D'ARIANO and L. MACCONE, unpublished.
[5] G. M. D'ARIANO and M. F. SACCHI, Phys. Rev. A **52** R4309 (1995).
[6] L. DIECI, B. MORINI, and A. PAPINI, Siam J. Matrix Anal. Appl. Vol. 17 **3**, 570 (1996); L. DIECI, B. MORINI, A. PAPINI, and A. PASQUALI, submitted to Applied Numerical Mathematics.
[7] C. GINZEL, M. J. BRIGEL, U. MARTINI, B. G. ENGLERT, and A. SCHENZLE, Phys. Rev. A **48**, 732 (1993).
[8] K. MØLMER, Y. CASTIN, and J. DALIBARD, J. Opt. Soc. Am. B **10**, 524 (1993); R. DUM, P. ZOLLER, and H. RITSCH, Phys. Rev. A **45**, 4879 (1992).
[9] KWIAT, STEINBERG, CHIAO, EBERHARD, and PETROFF, Phys. Rev. A **48**, 867 (1993); M. ATAC, Proc. of the SPIE Vol. 2007, 49 (1993); Peacock, Verhoeve, Rando, van Dordrecht, Taylor, Erd, Perryman, Venn, Howlett, Nature Vol. 381, no. 6578, 135 (1996).